CrossMark

ORIGINAL ARTICLE

A shallow water equation based on displacement and pressure and its numerical solution

Feng Wu[1] (iD) · **Wan-Xie Zhong**[1]

Abstract The primary purpose of this paper is to develop an efficient numerical scheme for solving the shallow water wave problem with a sloping water bottom and wet-dry interface. For this purpose, the Lagrange method and the constrained Hamilton variational principle are used to solve the shallow water wave problem. According to the constrained Hamilton variational principle, a shallow water equation based on the displacement and pressure (SWE-DP) is derived. Based on the discretized constrained Hamilton variational principle, a numerical scheme is developed for solving the SWE-DP. The proposed scheme combines the finite element method for spatial discretization and the simplectic Zu-class method for time integration. The correctness of the SWE-DP and the effectiveness of the proposed scheme are verified by three classical numerical examples. Numerical examples show that the proposed method performs well in the simulation of the shallow water problem with a sloping water bottom and wet-dry interface.

List of symbols

x, z	Spatial coordinates
t	Time
u, w	Displacements in x and y-axes
d	Water depth at time t
d_0	Water depth at the initial time
T, U	Kinetic and potential energies

✉ Feng Wu
  wufeng_chn@163.com

  Wan-Xie Zhong
  zwoffice@dlut.edu.cn

[1] State Key Laboratory of Structural Analysis of Industrial Equipment, Faculty of Vehicle Engineering and Mechanics, Dalian University of Technology, Dalian 116023, People's Republic of China

S	Action functional
g	Acceleration of gravity
n, k	Indexes

Greek symbols

η	Vertical displacement at the surface
φ	Vertical displacement at the bottom
(ξ, ζ)	Location of the particle at time t
ρ	Mass density
β	Pressure at the bottom
δ	Variational operator
Δx_n	Length of the nth element
Δt	Time step

1 Introduction

The theory of shallow water is widely applied in engineering such as in offshore engineering, ship engineering and environmental engineering; because of its importance, it has been studied extensively [1–3]. A great number of theoretical models have been proposed for simulating shallow water problems, such as the KdV equation, Saint–Venant equation (SVE) and Boussinesq equation [2, 4–7]. However, all these equations are based on the Eulerian coordinate system. The shallow water equations constructed using the Eulerian coordinate system consist of convective and source terms. The inclusion of the convective term means that the numerical scheme should be designed carefully. The most widely used numerical method for solving the Eulerian shallow water equations may be the finite volume method [8], because its discrete scheme can preserve the mass and momentum well. However, the source term often destroy the conservativeness of the finite volume method [9]. Moreover, the source term produced by the sloping water bottom often results in a numerical imbalance problem, i.e., the numerical still water cannot stay motionless [6, 10]. Numerical methods, which can preserve the motionless steady states, are often called well-balanced methods. The use of a numerical method that cannot preserve this property may lead to the spurious numerical waves [11]. The need for an adequate discretization of the topographical source term to preserve the "well-balanced" property has long been an important issue in computational shallow water dynamics [6, 10, 12]. Many researchers have developed well-balanced methods for the shallow water problems, see, for example, [10, 12–16]. Another difficult issue often encountered in the numerical approximation of the shallow water problem is how to address the wetting/drying condition. This issue is essentially a moving boundary problem and often leads to some numerical problems, such as mass loss and a negative water depth [17]. Because in the Euler framework the unknown variable is the flow velocity, it is inconvenient to exactly capture the transient position of the moving boundary, which involves the displacement of the water particles at the moving boundary.

The motion of water can also be described by the trajectories of particles that are carried along with the fluid flow. This description is commonly referred to as the Lagrange method [18]. In the Lagrange method, the displacements of the individual water particles are determined with respect to the time and the initial positions of the particles [19]. Using these displacements, the sloping water bottom and the moving boundary can be described exactly and easily [20, 21]. Motivated by this advantage, there have been many reports

discussing the use of the Lagrange method in hydrodynamics. In [20], Tao applied the Lagrangian coordinate system to discuss the sudden starting of a floating body in deep water. In [21], Tao and Shi applied the Lagrangian coordinate system to discuss the problem of the hydrodynamic pressure on a suddenly starting vessel. In [22], Shi employed the Lagrangian coordinate system to discuss a nonlinear wave induced by the acceleration of a cylindrical tank.

Using the Lagrange method, the nonlinear boundary condition on the free surface can be exactly satisfied [20–22]. By using the theory of classical mechanics, it is easy to establish the Hamilton variational principle for the hydrodynamics problem in the Lagrangian description. Finding the Hamilton variational principle for the hydrodynamics problem is undoubtedly important, and there have been many excellent works published on this topic [23–27]. Based on the Hamilton variational principle, numerical methods that have been successfully developed and widely applied in structural dynamics, such as the finite element method [28] and the symplectic method [29, 30], can be applied to simulate the shallow water problem. For a Hamilton system with the displacement $q(t)$ and momentum $p(t)$, the symplecticity means that $\mathrm{d}p(t) \wedge \mathrm{d}q(t) = \mathrm{d}p(0) \wedge \mathrm{d}q(0)$ holds for any time t. The symplecticity is the intrinsic geometric symmetry of the Hamilton dynamic system. If the algorithm can maintain the geometric symmetry of the symplecticity, it is called the symplectic method. The symplectic method can avoid the flaw of artificial dissipation and, hence, performs better than the traditional non-symplectic method, especially for problems that require extensive numerical simulation [29].

Recently, Wu and Zhong [31] proposed a constrained Hamilton variational principle for the shallow water problem. In the constrained Hamilton variational principle, the incompressible condition is treated as the constraint, and the pressure is seen as the Lagrangian multiplier. According to the constrained Hamilton variational principle, a shallow water equation based on displacement and pressure (SWE-DP) is developed. To numerically solve the SWE-DP, they developed a hybrid numerical method combining the finite element method for spatial discretization and the symplectic Zu-class method for time integration. Their method is symplectic and can preserve the total energy and mass of the shallow water system well. However, in Ref. [31], the authors only considered shallow water with an even bottom; the wetting/drying condition and the sloping water bottom were not discussed.

In this study, the theory proposed in Ref. [31] is extended to shallow water with a sloping bottom and wet-dry interface. In Sect. 2, a SWE-DP for the shallow water system with a sloping bottom and wet-dry interface is derived. In Sect. 3, a hybrid numerical scheme combining the finite element method for spatial discretization and the symplectic Zu-class method for time integration is established for the proposed SWE-DP. In Sect. 4, three classical numerical examples are evaluated to verify the correction of the proposed SWE-DP and the effectiveness of the proposed numerical scheme. In the last section, some conclusions are presented.

2 Shallow water equation based on displacement and pressure

Consider the shallow water model shown by Fig. 1. The water bottom is defined by $z + h(x) = 0$. The initial water surface is defined by $z - \eta_0(x) = 0$, while $u(x, z, t)$ and $w(x, z, t)$ represent the displacements of a certain particle in the water in the x- and
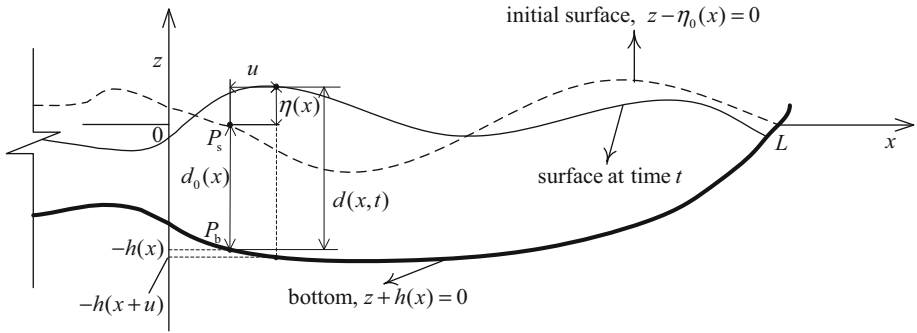
Fig. 1 The considered model with variable bottom topography

z-directions at time t, respectively. The particle is localized at (x, z) initially and at (ξ, ζ) at time t, where

$$\xi = x + u(x, z, t), \quad \zeta = z + w(x, z, t). \tag{1}$$

$d(x, t)$ represents the water depth at time t, and $d_0(x)$ the water depth at the initial time.

We assume that the water is inviscid and incompressible. Along the free surface, the pressure is zero, and the surface-energy effects are negligible. The need is to predict the evolution of water for $0 \le x \le L$. At $x = L$ is the wet-dry interface. The water depth at the wet-dry interface is zero, i.e., $d(L, t) = 0$. For $x = 0$, we suppose that the horizontal displacement $u(0, t)$, or the water depth $d(0, t)$, has been measured.

According to the theory of classical mechanics, the action of the water system in two space dimensions can be written as

$$S = \int_0^t (T - U + R) \mathrm{d}s, \tag{2}$$

where T, U and R are the kinetic energy, potential energy and constrained term, i.e.,

$$T = \int_0^L \int_{-h(x)}^{\eta_0(x)} \frac{1}{2} \rho (\dot{u}^2 + \dot{w}^2) \mathrm{d}z \mathrm{d}x, \tag{3}$$

$$U = \int_0^L \int_{-h(x)}^{\eta_0(x)} \rho g(z + w) \mathrm{d}z \mathrm{d}x, \tag{4}$$

and

$$R = \int_0^L \int_{-h(x)}^{\eta_0(x)} P\theta \mathrm{d}z \mathrm{d}x. \tag{5}$$

Here, P is the pressure, the dot represents the derivative with respect to time, and θ is the water volume strain, which can be written as

$$\theta = u_x + w_z + u_x w_z - u_z w_x. \tag{6}$$

For the shallow water problem, it can be assumed that the horizontal displacement is independent of the vertical coordinate z, i.e., $u(x, t) = u(x, z, t)$, and hence the water volume strain can be simplified as

$$\theta = u_x + w_z + u_x w_z. \tag{7}$$

According to the incompressible condition, the water volume strain should be rigorously zero $\theta = 0$, and hence we have

$$(1 + w_z)(1 + u_x) = 1, \quad \text{or} \quad w_z(x, z) = \frac{-u_x(x)}{1 + u_x(x)}. \tag{8}$$

Equation (8) shows that the vertical displacement distributes linearly along the vertical coordinate z. As shown in Fig. 1, the initial horizontal positions of the particle P_s at the surface and the particle P_b at the bottom are the same. Let the vertical displacements of particles P_b and P_s be denoted by

$$w(x, -h, t) = \varphi(x, t), \quad w(x, \eta_0, t) = \eta(x, t). \tag{9}$$

The vertical displacement can be written as

$$w(x, z, t) = \frac{z + h}{d_0} \eta(x, t) + \frac{\eta_0 - z}{d_0} \phi(x, t). \tag{10}$$

Taking the derivative of Eq. (10) with respect to z, and combining the result with Eq. (8) gives

$$w_z(x, z, t) = \frac{-u_x(x)}{1 + u_x(x)} = \frac{\eta(x, t) - \phi}{d_0}. \tag{11}$$

As shown in Fig. 1, the initial position of particle P_b at the bottom is $(x, -h(x))$, and its position at time t is $(x + u, -h(x + u))$. Hence, the vertical displacement is

$$\varphi(x, t) = h(x) - h(x + u). \tag{12}$$

Substituting Eq. (12) into Eq. (10) yields

$$w(x, z, t) = \frac{z + h}{d_0} d - z - h(x + u) \tag{13}$$

where $d(x, t)$ is the water depth at time t. $d(x, t)$ can be expressed as

$$d(x, t) = \eta(x, t) + h(x + u) + d_0(x) - h(x). \tag{14}$$

Substituting Eq. (13) into Eq. (4), the potential energy is rewritten as

$$U = \int_0^L \int_{-h(x)}^{\eta_0(x)} \rho g(z + w) \, dz \, dx = \frac{1}{2} \int_0^L \rho g d_0 d \, dx - \int_0^L \rho g d_0 h(x + u) \, dx. \tag{15}$$

In terms of Eq. (13), the vertical velocity is

$$\dot{w}(x, z, t) = \frac{z + h}{d_0} \dot{d}(x, t) - \bar{h}_x \dot{u}, \quad \bar{h}_x = \frac{\partial h(a)}{\partial a}\bigg|_{a = x + u} = h_x(x) + h_{xx}(x)u + \cdots. \tag{16}$$

For the shallow water problem, the nonlinear effect of the vertical velocity is negligible [32–34], and hence we make the approximation $\bar{h}_x \approx h_x(x)$ and obtain

$$\dot{w}(x, z, t) = \frac{z + h}{d_0}\dot{d}(x, t) - h_x(x)\dot{u}. \tag{17}$$

Then, substituting Eq. (17) into Eq. (3) yields

$$T = \frac{1}{2}\int_0^L \int_{-h(x)}^{\eta_0(x)} \rho(\dot{u}^2 + \dot{w}^2)\mathrm{d}z\mathrm{d}x = T_1 + T_2, \tag{18}$$

where

$$T_1 = \frac{1}{2}\int_0^L (\rho d_0\dot{u}^2)\mathrm{d}x, \quad T_2 = \frac{1}{2}\int_0^L \rho\left(\frac{d_0}{3}\dot{d}^2 - d_0 h_x\dot{u}\dot{d} + d_0 h_x^2\dot{u}^2\right)\mathrm{d}x. \tag{19}$$

Here, T_1 represents the kinetic energy produced by the horizontal velocity and T_2 the kinetic energy produced by the vertical velocity. In the shallow water long wave problem, T_2 is negligible relative to T_1 [19, 35].

The pressure at the water surface is zero. Let the pressure at the bottom be denoted by

$$P(x, -h(x), t) = \beta(x, t). \tag{20}$$

Making an assumption that the pressure distributes linearly along the vertical coordinate z, we have

$$P(x, z, t) = \frac{\eta_0 - z}{d_0}\beta(x, t). \tag{21}$$

Substituting Eq. (13) into the expression (7) of the water volume strain yields

$$\theta = u_x + (1 + u_x)\left(\frac{d}{d_0} - 1\right). \tag{22}$$

Substituting Eqs. (21) and (22) into Eq. (5) yields

$$R = \frac{1}{2}\int_0^L \beta[d(1 + u_x) - d_0]\mathrm{d}x. \tag{23}$$

In terms of Eqs. (15), (18) and (23), the action of the shallow water system can be written as

$$\begin{aligned}
S = &\frac{1}{2}\int_0^t \int_0^L \rho\left(d_0\dot{u}^2 + \frac{d_0}{3}\dot{d}^2 - d_0 h_x\dot{u}\dot{d} + d_0 h_x^2\dot{u}^2\right)\mathrm{d}x\mathrm{d}s - \int_0^t \frac{1}{2}\int_0^L \rho g d_0 d\,\mathrm{d}x\mathrm{d}s \\
&+ \int_0^t \int_0^L \rho g d_0 h(x + u)\mathrm{d}x\mathrm{d}s + \frac{1}{2}\int_0^t \int_0^L \beta[d(1 + u_x) - d_0]\mathrm{d}x\mathrm{d}s.
\end{aligned} \tag{24}$$

The action S is a functional based on u, d and β. According to the Hamilton variational principle, the true solution, i.e., (u, d, β), is the stationary point of the action functional. Taking the first variation of the action S with respect to (u, d, β) yields

$$\delta S = \frac{1}{2}\int_0^t \int_0^L \rho \left[\begin{array}{l} d_0 2(\delta \dot{u})\dot{u} + \dfrac{d_0}{3}2(\delta \dot{d})\dot{d} - d_0 h_x(\delta \dot{u})\dot{d} \\[2mm] - d_0 h_x \dot{u}(\delta \dot{d}) + d_0 h_x^2 2(\delta \dot{u})\dot{u} \end{array} \right] \mathrm{d}x\mathrm{d}s$$

$$- \int_0^t \frac{1}{2}\int_0^L \rho g d_0 \delta d \ \mathrm{d}x\mathrm{d}s + \int_0^t \int_0^L \rho g d_0 \bar{h}_x(\delta u)\mathrm{d}x\mathrm{d}s \tag{25}$$

$$+ \frac{1}{2}\int_0^t \int_0^L \beta[(\delta d)(1 + u_x)]\mathrm{d}x\mathrm{d}s + \frac{1}{2}\int_0^t \int_0^L (\delta \beta)[d(1 + u_x) - d_0]\mathrm{d}x\mathrm{d}s$$

$$+ \frac{1}{2}\int_0^t \int_0^L \beta d(\delta u_x)\mathrm{d}x\mathrm{d}s$$

where δ represents the variational operator. According to classical mechanics, δu, δd and $\delta \beta$ in Eq. (25) are arbitrary function, which can be called the virtual displacement, virtual depth, and virtual pressure, respectively. Applying integration by parts to the first integral term on right-hand side of Eq. (25), we have

$$\frac{1}{2}\int_0^t \int_0^L \rho[d_0 2(\delta \dot{u})\dot{u}]\mathrm{d}x\mathrm{d}s$$
$$= \int_0^L \rho d_0 \left[\int_0^t (\delta \dot{u})\dot{u}\mathrm{d}s \right]\mathrm{d}x = \int_0^L \rho d_0 \left[\int_0^t \dot{u}\mathrm{d}(\delta u) \right]\mathrm{d}x \tag{26}$$
$$= \int_0^L \rho d_0 [\dot{u}(\delta u)]_0^t \mathrm{d}x - \int_0^L \rho d_0 \left[\int_0^t (\delta u)\ddot{u}\mathrm{d}s \right]\mathrm{d}x.$$

If the horizontal displacement at times 0 and t are given, that is, $\delta u(x,0) = \delta u(x,t) = 0$ which causes the first term on the right-hand side of Eq. (26) to vanish, we have

$$\frac{1}{2}\int_0^t \int_0^L \rho[d_0 2(\delta \dot{u})\dot{u}] \ \mathrm{d}x\mathrm{d}s = - \int_0^L \rho d_0 \left[\int_0^t (\delta u)\ddot{u}\mathrm{d}s \right]\mathrm{d}x. \tag{27}$$

Analogously, if the water depth d at times 0 and t are given, we have

$$\frac{1}{2}\int_0^t \int_0^L \rho \left[\begin{array}{l} d_0 2(\delta \dot{u})\dot{u} + \dfrac{d_0}{3}2(\delta \dot{d})\dot{d} - d_0 h_x(\delta \dot{u})\dot{d} \\[2mm] -d_0 h_x \dot{u}(\delta \dot{d}) + d_0 h_x^2 2(\delta \dot{u})\dot{u} \end{array} \right] \mathrm{d}x\mathrm{d}s$$
$$= \frac{1}{2}\int_0^t \int_0^L \rho \left(-2(\delta u)d_0\ddot{u} - 2(\delta d)\frac{d_0}{3}\ddot{d} + d_0 h_x(\delta u)\ddot{d} + d_0 h_x \ddot{u}(\delta d) - 2(\delta u)d_0 h_x^2 \ddot{u} \right)\mathrm{d}x\mathrm{d}s \tag{28}$$

Applying integration by parts to the last integral term on right-hand side of Eq. (25), we have

$$\frac{1}{2}\int_0^t \int_0^L \beta d(\delta u_x)\mathrm{d}x\mathrm{d}s = \frac{1}{2}\int_0^t \left[\int_0^L \beta d\mathrm{d}(\delta u) \right]\mathrm{d}s$$
$$= \frac{1}{2}\int_0^t \left[[\beta d(\delta u)]_{x=0}^{x=L} - \int_0^L (\delta u)\frac{\partial(\beta d)}{\partial x}\mathrm{d}x \right]\mathrm{d}s \tag{29}$$
$$= -\frac{1}{2}\int_0^t \int_0^L \frac{\partial(\beta d)}{\partial x}\delta u\mathrm{d}x\mathrm{d}s + \frac{1}{2}\int_0^t [\beta d\delta u]_{x=0}^{x=L}\mathrm{d}s.$$

Substituting Eqs. (28) and (29) into Eq. (25) yields

$$
\begin{aligned}
\delta S = {} & \frac{1}{2}\int_0^t\int_0^L \rho\left(-2\delta u d_0\ddot{u} - 2\delta d\frac{d_0}{3}\ddot{d} + d_0 h_x\delta u\ddot{d} + d_0 h_x\ddot{u}\delta d - 2\delta u d_0 h_x^2\ddot{u}\right)\mathrm{d}x\mathrm{d}s \\
& -\int_0^t\frac{1}{2}\int_0^L \rho g d_0\delta d\mathrm{d}x\mathrm{d}s + \int_0^t\int_0^L \rho g d_0\bar{h}_x\delta u\mathrm{d}x\,\mathrm{d}s \\
& +\frac{1}{2}\int_0^t\int_0^L \beta\delta d(1+u_x)\mathrm{d}x\,\mathrm{d}s + \frac{1}{2}\int_0^t\int_0^L \delta\beta[d(1+u_x)-d_0]\mathrm{d}x\,\mathrm{d}s \\
& -\frac{1}{2}\int_0^t\int_0^L \frac{\partial(\beta d)}{\partial x}\delta u\mathrm{d}x\,\mathrm{d}s + \frac{1}{2}\int_0^t [\beta d\delta u]_{x=0}^{x=L}\mathrm{d}s
\end{aligned}
\tag{30}
$$

Noting that the water depth at the wet-dry interface is rigorously zero, that is $d(L, s) = 0$, if the horizontal displacement at $x = 0$ is given, we have

$$
\delta u(0, s) = 0, \quad 0 \le s \le t.
\tag{31}
$$

Hence the last term on the right-hand side of Eq. (30) equals to zero. The right-hand side of Eq. (30) can thus be rewritten as

$$
\begin{aligned}
\delta S = {} & \int_0^t\int_0^L (-\delta u)\left(\rho d_0\ddot{u} - \frac{1}{2}\rho d_0 h_x\ddot{d} + \rho d_0 h_x^2\ddot{u} - \rho g d_0\bar{h}_x + \frac{1}{2}\frac{\partial(\beta d)}{\partial x}\right)\mathrm{d}x\mathrm{d}s \\
& +\int_0^t\int_0^L (-\delta d)\left(\rho\frac{d_0}{3}\ddot{d} - \frac{1}{2}\rho d_0 h_x\ddot{u} + \frac{1}{2}\rho g d_0 - \frac{1}{2}\beta(1+u_x)\right)\mathrm{d}x\mathrm{d}s \\
& +\frac{1}{2}\int_0^t\int_0^L (\delta\beta)[d(1+u_x)-d_0]\mathrm{d}x\mathrm{d}s
\end{aligned}
\tag{32}
$$

Noting that the virtual functions δu, δd and $\delta\beta$ are arbitrary, we obtain

$$
\begin{cases}
\rho d_0\ddot{u} - \dfrac{1}{2}\rho d_0 h_x\ddot{d} + \rho d_0 h_x^2\ddot{u} - \rho g d_0\bar{h}_x + \dfrac{1}{2}\dfrac{\partial(\beta d)}{\partial x} = 0 \\
\rho\dfrac{d_0}{3}\ddot{d} - \dfrac{1}{2}\rho d_0 h_x\ddot{u} + \dfrac{1}{2}\rho g d_0 - \dfrac{1}{2}\beta(1+u_x) = 0 \\
d(1+u_x) = d_0,
\end{cases}
\tag{33}
$$

which is the shallow water equation based on displacement and pressure (SWE-DP). The third equation in Eq. (33) is the incompressible condition of the shallow water system.

In the above steps from Eq. (30) to (32), we use the boundary condition $\delta u(x, s) = 0$ for $0 \le s \le t$, which holds on only when the horizontal displacement at $x = 0$ is given. If boundary condition at $x = 0$ is replaced with giving the water depth $d(0, s)$ for $0 \le s \le t$, introduce the following force

$$
f(s) = \frac{1}{2}\beta d(0, s), \quad 0 \le s \le t
\tag{34}
$$

which is actually a pressure applied at $x = 0$. In this case, the potential energy should be modified to

$$
U = \frac{1}{2}\int_0^L \rho g d_0 d\mathrm{d}x - \int_0^L \rho g d_0 h(x+u)\mathrm{d}x - fu(0, s).
\tag{35}
$$

Correspondingly, the action should be modified to

$$
\begin{aligned}
S = {} & \frac{1}{2} \int_0^t \int_0^L \rho \left(d_0 \dot{u}^2 + \frac{d_0}{3} \dot{d}^2 - d_0 h_x \dot{u} \dot{d} + d_0 h_x^2 \dot{u}^2 \right) \mathrm{d}x\mathrm{d}s - \int_0^t \frac{1}{2} \int_0^L \rho g d_0 d \, \mathrm{d}x\mathrm{d}s \\
& + \int_0^t \int_0^L \rho g d_0 h(x + u) \mathrm{d}x\mathrm{d}s + \frac{1}{2} \int_0^t \int_0^L \beta[d(1 + u_x) - d_0] \mathrm{d}x\mathrm{d}s + \int_0^t f u(0, s) \mathrm{d}s
\end{aligned}
\tag{36}
$$

Taking the first variation of S, and setting $\delta S = 0$ will yield Eqs. (33) and (34).

If the effect of the vertical velocity is ignored, the kinetic energy is T_1, and the SWE-DP (33) can be simplified as

$$
\begin{cases}
\rho d_0 \ddot{u} - \rho g d_0 \bar{h}_x + \dfrac{1}{2} \dfrac{\partial(\beta d)}{\partial x} = 0 \\
\rho g d_0 - \beta(1 + u_x) = 0 \\
d(1 + u_x) = d_0
\end{cases}
\tag{37}
$$

Combining the second and third equations in Eq. (37), we obtain

$$
\beta = \frac{\rho g d_0}{1 + u_x} = \rho g d.
\tag{38}
$$

Noting that β is the pressure at the water bottom and d is the water depth, Eq. (38) reflects the assumption of the hydrostatic pressure, which is the fundamental assumption in the SVE. Indeed, Eq. (37) is mathematically equivalent to the SVE, which will be proven in the appendix. Hence, some analytical solutions to the SVE can be employed to test the validity of the numerical scheme to the SWE-DP proposed in the next section.

3 Numerical scheme

The proposed SWE-DP is nonlinear, and it is hard to solve this equation by purely analytical methods. In this section, with the help of the discretized constrained Hamilton variational principle, a hybrid method combining the finite element for the spatial discretization and the symplectic Zu-class method for the time integration is presented for this equation.

3.1 Discretization in space

The proposed SWE-DP (33) is derived in terms of the constrained Hamilton variational principle. Hence, it is a natural choice to use the finite element method for spatial discretization. Let the region $[0, L]$ be divided into N_e basic elements with N_d nodes; see Fig. 2.

On the nth element, the horizontal displacement $u(x)$ is approximated by the linear function, and $d(x)$ and $\beta(x)$ are treated as constant values, i.e.,

$$
u(x) = \frac{x_{n+1} - x}{\Delta x_n} u_n + \frac{x - x_n}{\Delta x_n} u_{n+1}, \quad d(x) = d_n, \quad \beta(x) = \beta_n,
\tag{39}
$$

where x_n is the node location on the x-axis, Δx_n is the length of the nth element, u_n is the horizontal displacement of the nth node, d_n is the water depth evaluated at the mid-point of

the nth element, and β_n is the pressure of the water bottom evaluated at the mid-point of the nth element. In terms of Eqs. (33) and (39), the incompressible condition on the nth element can be approximated as

$$d_n \Delta x_n \left(1 + \frac{u_{n+1} - u_n}{\Delta x_n} \right) = \Delta x_n d_{0,n}. \tag{40}$$

The kinetic energy can be approximated as

$$T = \frac{1}{2} \dot{\mathbf{u}}^{\mathrm{T}} \mathbf{M}_u \dot{\mathbf{u}} + \frac{1}{2} \dot{\mathbf{d}}^{\mathrm{T}} \mathbf{M}_d \dot{\mathbf{d}} - \dot{\mathbf{d}}^{\mathrm{T}} \mathbf{M}_{du} \dot{\mathbf{u}}, \tag{41}$$

in which

$$\rho_u = \rho d_0 \left(1 + h_x^2 \right), \quad \rho_d = \frac{\rho d_0}{3}, \quad \rho_{ud} = \rho h_x d_0, \tag{42}$$

$$\mathbf{u} = \begin{pmatrix} u_1 & u_2 & \dots & u_{N_d} \end{pmatrix}^{\mathrm{T}}, \quad \mathbf{d} = \begin{pmatrix} d_1 & d_2 & \dots & d_{N_e} \end{pmatrix}^{\mathrm{T}}$$

$$\mathbf{M}_u = \mathrm{diag}\{ M_{u,1} \quad \dots \quad M_{u,n} \quad \dots \quad M_{u,N_d} \}$$

$$\mathbf{M}_d = \mathrm{diag}\{ \rho_{d,1} \Delta x_1 \quad \rho_{d,2} \Delta x_2 \quad \dots \quad \rho_{d,N_e} \Delta x_{N_e} \}$$

$$\mathbf{M}_{du} = \frac{1}{4} \begin{bmatrix} \Delta x_1 \rho_{ud,1} & \Delta x_1 \rho_{ud,1} & 0 & \cdots & 0 \\ 0 & \Delta x_2 \rho_{ud,2} & \Delta x_2 \rho_{ud,2} & \ddots & \vdots \\ \vdots & \ddots & \ddots & \ddots & 0 \\ 0 & \cdots & 0 & \Delta x_{N_e} \rho_{ud,N_e} & \Delta x_{N_e} \rho_{ud,N_e} \end{bmatrix}, \tag{43}$$

and

$$M_{u,1} = \frac{\Delta x_1 \rho_{u,1}}{2}, \quad M_{u,n} = \frac{\Delta x_{n-1} \rho_{u,n-1} + \Delta x_n \rho_{u,n}}{2}, \quad M_{u,N_d} = \frac{\Delta x_{N_e} \rho_{u,N_e}}{2}$$

$$\rho_{u,n} = \rho_u \left(\frac{x_n + x_{n+1}}{2} \right), \quad \rho_{d,n} = \rho_d \left(\frac{x_n + x_{n+1}}{2} \right), \quad \rho_{ud,n} = \rho_{ud} \left(\frac{x_n + x_{n+1}}{2} \right). \tag{44}$$

The potential energy can be approximated as

$$U = \mathbf{g}_d^{\mathrm{T}} \mathbf{d} - \mathbf{g}_h^{\mathrm{T}} \mathbf{h} \tag{45}$$

where

Fig. 2 The finite element mesh

$$\mathbf{g}_h^{\mathrm{T}} = \left(\frac{\Delta x_1}{2} g_{u,1}, \left(\frac{\Delta x_n}{2} + \frac{\Delta x_{n-1}}{2} \right) g_{u,n}, \frac{\Delta x_{N_e}}{2} g_{u,N_d} \right)^{\mathrm{T}}$$

$$\mathbf{g}_d^{\mathrm{T}} = \left(\frac{(g_{d,1} + g_{d,2}) \Delta x_1}{2} \quad \frac{(g_{d,2} + g_{d,3}) \Delta x_2}{2} \quad \cdots \quad \frac{(g_{d,N_d-1} + g_{d,N_d}) \Delta x_{N_e}}{2} \right)^{\mathrm{T}} \tag{46}$$

$$\mathbf{h}^{\mathrm{T}} = (h(x_1 + u_1), h(x_n + u_n), h(x_{N_d} + u_{N_d}))^{\mathrm{T}}$$

$$g_{d,n} = \frac{\rho g}{2} d_0(x_n), \quad g_{u,n} = \rho g d_0(x_n).$$

The Lagrangian modified term can be approximated as

$$R = 0.5 \boldsymbol{\beta}^{\mathrm{T}} \Delta \mathbf{d} + 0.5 \mathbf{d}^{\mathrm{T}} \mathbf{BCu} - 0.5 \boldsymbol{\beta}^{\mathrm{T}} \mathbf{s} \; = 0.5 \boldsymbol{\beta}^{\mathrm{T}} \Delta \mathbf{d} + 0.5 \boldsymbol{\beta}^{\mathrm{T}} \mathbf{DCu} - 0.5 \boldsymbol{\beta}^{\mathrm{T}} \mathbf{s} \tag{47}$$

where

$$\mathbf{s}^{\mathrm{T}} = \begin{pmatrix} \Delta x_1 d_{0,1} & \Delta x_n d_{0,2} & \Delta x_{N_e} d_{0,N_e} \end{pmatrix}$$

$$\mathbf{D} = \mathrm{diag}\{\mathbf{d}\}, \quad \Delta = \mathrm{diag}\{\Delta x_1, \Delta x_2, \ldots\}$$

$$\boldsymbol{\beta}^{\mathrm{T}} = \begin{pmatrix} \beta_1 & \beta_2 & \cdots & \beta_{N_e} \end{pmatrix}, \quad \mathbf{B} = \mathrm{diag}\{\boldsymbol{\beta}\} \tag{48}$$

$$\mathbf{C} = \begin{bmatrix} -1 & 1 & 0 & \cdots & 0 \\ 0 & -1 & 1 & \ddots & \vdots \\ \vdots & \ddots & \ddots & \ddots & 0 \\ 0 & \cdots & 0 & -1 & 1 \end{bmatrix}.$$

In terms of Eqs. (41), (45) and (47), the action can be approximated as

$$S = \int_0^t \left[\begin{array}{c} \frac{1}{2} \dot{\mathbf{u}}^{\mathrm{T}} \mathbf{M}_u \dot{\mathbf{u}} + \frac{1}{2} \dot{\mathbf{d}}^{\mathrm{T}} \mathbf{M}_d \dot{\mathbf{d}} - \dot{\mathbf{d}}^{\mathrm{T}} \mathbf{M}_{du} \dot{\mathbf{u}} - \mathbf{g}_d^{\mathrm{T}} \mathbf{d} + \mathbf{g}_h^{\mathrm{T}} \mathbf{h} \\ + \frac{1}{2} \boldsymbol{\beta}^{\mathrm{T}} \Delta \mathbf{d} + \frac{1}{2} \boldsymbol{\beta}^{\mathrm{T}} \mathbf{DCu} - \frac{1}{2} \boldsymbol{\beta}^{\mathrm{T}} \mathbf{s} \end{array} \right] \mathrm{d}s, \tag{49}$$

in which $\mathbf{u}$ and $\mathbf{d}$ are the horizontal displacement vector and the water depth vector, respectively, and $\boldsymbol{\beta}$ is the bottom pressure vector.

In the integrand of Eq. (49), the summation of the first three terms represents the kinetic energy, the summation of the fourth and fifth terms represents the potential energy, and the summation of the last three terms represents the constrained term.

According to the constrained Hamilton variational principle, $\delta S = 0$. If $\mathbf{u}$ and $\mathbf{d}$ at times 0 and t are given, i.e., $\delta \mathbf{u}(0) = \delta \mathbf{u}(t) = \mathbf{0}$ and $\delta \mathbf{d}(0) = \delta \mathbf{d}(t) = \mathbf{0}$, $\delta S = 0$ causes the following equations:

$$\begin{cases} \mathbf{M}_u \ddot{\mathbf{u}} - \mathbf{M}_{du}^{\mathrm{T}} \ddot{\mathbf{d}} - \mathbf{h}_{\mathbf{x}} \mathbf{g}_h - 0.5 \mathbf{C}^T \mathbf{Bd} = \mathbf{0} \\ \mathbf{M}_d \ddot{\mathbf{d}} - \mathbf{M}_{du} \ddot{\mathbf{u}} + \mathbf{g}_d - 0.5 \Delta \boldsymbol{\beta} - 0.5 \mathbf{BCu} = \mathbf{0} , \\ \Delta d + \mathbf{DCu} - \mathbf{s} = \mathbf{0} \end{cases} \tag{50}$$

which constitutes a system of differential algebraic equations (DAEs).

3.2 The Zu-class method

The nonlinear DAEs (50) are obtained from the first variation of Eq. (49), which corresponds to a constrained Hamiltonian system. For the Hamiltonian system, the symplecticity

is a characteristic property [29]. As the symplectic method can preserve the property of symplecticity and the approximate energy necessary for a long time computation, it often is preferable to simulate the Hamiltonian dynamical system [27]. However, for the constrained Hamiltonian system, it is required for a time integration method to preserve not only the symplectic structure of the Hamiltonian system but also all the constraints. In Ref. [36], a method preserving all the constraints was developed by Zhong et al. The numerical experiment of the double pendulum presented in [36] shows that this method can preserve energy well. In Ref. [37], it was named the Zu-class method. In Ref. [38], this method was proven to be symplectic. The symplectic Zu-class method is based on the discretized Hamilton variational principle. In the symplectic Zu-class method, the constraint conditions are satisfied strictly at the integration points, and the orbit is treated as geodesic in the state space and is therefore approximated by using the time finite element method. In this sub-section, the symplectic Zu-class method will be employed to solve the DAEs (50).

In the steps from Eq. (49) to Eq. (50), $\mathbf{u}$ and $\mathbf{d}$ at times 0 and t are assumed to be known, which causes $\delta\mathbf{u}(0) = \delta\mathbf{u}(t) = \mathbf{0}$ and $\delta\mathbf{d}(0) = \delta\mathbf{d}(t) = \mathbf{0}$. However this assumption is unnecessary according to classical mechanics [31, 35, 39]. Let action (49) be modified as

$$
\begin{aligned}
S = \int_0^t & \left[\begin{array}{l} \frac{1}{2}\dot{\mathbf{u}}^{\mathrm{T}}\mathbf{M}_u\dot{\mathbf{u}} + \frac{1}{2}\dot{\mathbf{d}}^{\mathrm{T}}\mathbf{M}_d\dot{\mathbf{d}} - \dot{\mathbf{d}}^{\mathrm{T}}\mathbf{M}_{du}\dot{\mathbf{u}} - \mathbf{g}_d^{\mathrm{T}}\mathbf{d} + \mathbf{g}_h^{\mathrm{T}}\mathbf{h} \\ + \frac{1}{2}\boldsymbol{\beta}^{\mathrm{T}}\Delta\mathbf{d} + \frac{1}{2}\boldsymbol{\beta}^{\mathrm{T}}\mathbf{DCu} - \frac{1}{2}\boldsymbol{\beta}^{\mathrm{T}}\mathbf{s} \end{array} \right] \mathrm{d}s \\
& + \mathbf{u}^{\mathrm{T}}(0)\mathbf{p}_u(0) - \mathbf{u}^{\mathrm{T}}(t)\mathbf{p}_u(t) \\
& + \mathbf{d}^{\mathrm{T}}(0)\mathbf{p}_d(0) - \mathbf{d}^{\mathrm{T}}(t)\mathbf{p}_d(t)
\end{aligned}
\tag{51}
$$

where $\mathbf{p}_u(t)$ and $\mathbf{p}_d(t)$ are the momentum vectors. Letting the first variation of Eq. (51) be zero will not yields Eq. (50), but rahter the following equation:

$$
\mathbf{p}_u = \mathbf{M}_u\dot{\mathbf{u}} - \mathbf{M}_{du}^{\mathrm{T}}\dot{\mathbf{d}}, \quad \mathbf{p}_d = \mathbf{M}_d\dot{\mathbf{d}} - \mathbf{M}_{du}\dot{\mathbf{u}}.
\tag{52}
$$

The Zu-class method is based on Eq. (51). Let the time domain be discretized as

$$
t = t_0, \ t_1, \ldots, t_k, \ldots, \quad t_k = k \times \Delta t,
\tag{53}
$$

where Δt is the time step, which should be limited by the usual CFL (Courant–Friedrichs–Lewy) condition [1, 3] to guarantee the convergence of the numerical results. Let the velocities in $[t_k,\ t_{k+1}]$ be approximated as

$$
\dot{\mathbf{u}}_k(t) = \frac{\mathbf{u}_{k+1} - \mathbf{u}_k}{\Delta t}, \quad \dot{\mathbf{d}}_k(t) = \frac{\mathbf{d}_{k+1} - \mathbf{d}_k}{\Delta t}, \quad t \in [t_k,\ t_{k+1}],
\tag{54}
$$

where $\#_k = \#(t_k)$, and the displacements be approximated as

$$
\mathbf{u}(t) = \frac{\mathbf{u}_{k+1} + \mathbf{u}_k}{2}, \quad \mathbf{d}(t) = \frac{\mathbf{d}_{k+1} + \mathbf{d}_k}{2}, \quad t \in [t_k,\ t_{k+1}].
\tag{55}
$$

The bottom pressure is approximated to be a constant in $[t_k,\ t_{k+1}]$, i.e.,

$$
\boldsymbol{\beta}(t) = \boldsymbol{\beta}_k, \quad t \in [t_k,\ t_{k+1}].
\tag{56}
$$

In terms of Eqs. (51), and (54)–(56), the action for $t \in [t_k,\ t_{k+1}]$ can be written as

$$S = \int_{t_k}^{t_{k+1}} T \mathrm{d}s - \int_{t_k}^{t_{k+1}} U \mathrm{d}s + \int_{t_k}^{t_{k+1}} R \mathrm{d}s + \mathbf{u}_k^{\mathrm{T}} \mathbf{p}_{u,k} - \mathbf{u}_{k+1}^{\mathrm{T}} \mathbf{p}_{u,k+1} + \mathbf{d}_k^{\mathrm{T}} \mathbf{p}_{d,k} - \mathbf{d}_{k+1}^{\mathrm{T}} \mathbf{p}_{d,k+1}$$

(57)

where

$$\int_{t_k}^{t_{k+1}} T \mathrm{d}s = \frac{1}{2} \left(\mathbf{u}_{k+1}^{\mathrm{T}} - \mathbf{u}_k^{\mathrm{T}} \right) \mathbf{M}_u \left(\frac{\mathbf{u}_{k+1} - \mathbf{u}_k}{\Delta t} \right) + \frac{1}{2} \left(\mathbf{d}_{k+1}^{\mathrm{T}} - \mathbf{d}_k^{\mathrm{T}} \right) \mathbf{M}_d \frac{\mathbf{d}_{k+1} - \mathbf{d}_k}{\Delta t}$$
$$\qquad - \left(\mathbf{d}_{k+1}^{\mathrm{T}} - \mathbf{d}_k^{\mathrm{T}} \right) \mathbf{M}_{du} \left(\frac{\mathbf{u}_{k+1} - \mathbf{u}_k}{\Delta t} \right)$$
$$\int_{t_k}^{t_{k+1}} U \mathrm{d}s = \frac{\Delta t}{2} \mathbf{g}_d^{\mathrm{T}} (\mathbf{d}_k + \mathbf{d}_{k+1}) - \frac{\Delta t}{2} \mathbf{g}_h^{\mathrm{T}} [\mathbf{h}(\mathbf{u}_k) + \mathbf{h}(\mathbf{u}_{k+1})]$$
$$\int_{t_k}^{t_{k+1}} R \mathrm{d}s = \frac{1}{2} \boldsymbol{\beta}_k^{\mathrm{T}} \boldsymbol{\Delta} \frac{\Delta t}{2} (\mathbf{d}_k + \mathbf{d}_{k+1}) + \frac{1}{2} \boldsymbol{\beta}_k^{\mathrm{T}} \frac{\Delta t}{2} (\mathbf{D}_k \mathbf{C} \mathbf{u}_k + \mathbf{D}_{k+1} \mathbf{C} \mathbf{u}_{k+1}) - \frac{1}{2} \Delta t \boldsymbol{\beta}_k^{\mathrm{T}} \mathbf{s}$$

(58)

Substituting Eq. (58) into the action integral and taking the first variation gives

$$\delta S = \delta \left(\mathbf{u}_{k+1}^{\mathrm{T}} - \mathbf{u}_k^{\mathrm{T}} \right) \mathbf{M}_u \left(\frac{\mathbf{u}_{k+1} - \mathbf{u}_k}{\Delta t} \right) + \delta \left(\mathbf{d}_{k+1}^{\mathrm{T}} - \mathbf{d}_k^{\mathrm{T}} \right) \mathbf{M}_d \frac{\mathbf{d}_{k+1} - \mathbf{d}_k}{\Delta t}$$
$$\quad - \delta \left(\mathbf{d}_{k+1}^{\mathrm{T}} - \mathbf{d}_k^{\mathrm{T}} \right) \mathbf{M}_{du} \left(\frac{\mathbf{u}_{k+1} - \mathbf{u}_k}{\Delta t} \right) - \delta \left(\mathbf{u}_{k+1}^{\mathrm{T}} - \mathbf{u}_k^{\mathrm{T}} \right) \mathbf{M}_{du}^{\mathrm{T}} \left(\frac{\mathbf{d}_{k+1} - \mathbf{d}_k}{\Delta t} \right)$$
$$\quad - \left[\frac{\Delta t}{2} \delta \left(\mathbf{d}_k^{\mathrm{T}} + \mathbf{d}_{k+1}^{\mathrm{T}} \right) \mathbf{g}_d - \frac{\Delta t}{2} \left(\delta \mathbf{u}_k^{\mathrm{T}} \mathbf{h}_{\mathbf{u}_k} \mathbf{g}_h + \delta \mathbf{u}_{k+1}^{\mathrm{T}} \mathbf{h}_{\mathbf{u}_{k+1}} \mathbf{g}_h \right) \right]$$
$$\quad + \left(\delta \boldsymbol{\beta}_k^{\mathrm{T}} \right) \frac{\Delta t}{4} \boldsymbol{\Delta} (\mathbf{d}_k + \mathbf{d}_{k+1}) + \delta \left(\mathbf{d}_k^{\mathrm{T}} + \mathbf{d}_{k+1}^{\mathrm{T}} \right) \frac{\Delta t}{4} \boldsymbol{\Delta} \boldsymbol{\beta}_k$$
$$\quad + \left(\delta \boldsymbol{\beta}_k^{\mathrm{T}} \right) \frac{\Delta t}{4} (\mathbf{D}_k \mathbf{C} \mathbf{u}_k + \mathbf{D}_{k+1} \mathbf{C} \mathbf{u}_{k+1}) + \frac{\Delta t}{4} \left[(\delta \mathbf{d}_k^{\mathrm{T}}) \mathbf{B}_k \mathbf{C} \mathbf{u}_k + (\delta \mathbf{d}_{k+1}^{\mathrm{T}}) \mathbf{B}_k \mathbf{C} \mathbf{u}_{k+1} \right]$$
$$\quad + \frac{\Delta t}{4} \left[(\delta \mathbf{u}_k^{\mathrm{T}}) \mathbf{C}^{\mathrm{T}} \mathbf{D}_k \boldsymbol{\beta}_k + (\delta \mathbf{u}_{k+1}^{\mathrm{T}}) \mathbf{C}^{\mathrm{T}} \mathbf{D}_{k+1} \boldsymbol{\beta}_k \right] - (\delta \boldsymbol{\beta}_k^{\mathrm{T}}) \frac{1}{2} \Delta t \mathbf{s}$$
$$\quad + \delta \mathbf{u}_k^{\mathrm{T}} \mathbf{p}_{u,k} - \delta \mathbf{u}_{k+1}^{\mathrm{T}} \mathbf{p}_{u,k+1} + \delta \mathbf{d}_k^{\mathrm{T}} \mathbf{p}_{d,k} - \delta \mathbf{d}_{k+1}^{\mathrm{T}} \mathbf{p}_{d,k+1}$$

(59)

where

$$\mathbf{h}_{\mathbf{u}_k} = \frac{\partial \mathbf{h}^{\mathrm{T}}(\mathbf{u}_k)}{\partial \mathbf{u}_k}, \quad \mathbf{h}_{\mathbf{u}_{k+1}} = \frac{\partial \mathbf{h}^{\mathrm{T}}(\mathbf{u}_{k+1})}{\partial \mathbf{u}_{k+1}}$$

(60)

Equation (59) can be further simplified as

$$\delta S = \left(\delta \mathbf{u}_{k+1}^{\mathrm{T}}\right)\left[\mathbf{M}_u\left(\frac{\mathbf{u}_{k+1}-\mathbf{u}_k}{\Delta t}\right)-\mathbf{M}_{du}^{\mathrm{T}}\left(\frac{\mathbf{d}_{k+1}-\mathbf{d}_k}{\Delta t}\right)+\frac{\Delta t}{2}\mathbf{h}_{\mathbf{u}_{k+1}}\mathbf{g}_h+\frac{\Delta t}{4}\mathbf{C}^{\mathrm{T}}\mathbf{D}_{k+1}\boldsymbol{\beta}-\mathbf{p}_{u,k+1}\right]$$

$$+\left(\delta \mathbf{u}_k^{\mathrm{T}}\right)\left[-\mathbf{M}_u\left(\frac{\mathbf{u}_{k+1}-\mathbf{u}_k}{\Delta t}\right)+\mathbf{M}_{du}^{\mathrm{T}}\left(\frac{\mathbf{d}_{k+1}-\mathbf{d}_k}{\Delta t}\right)+\frac{\Delta t}{2}\mathbf{h}_{\mathbf{u}_k}\mathbf{g}_h+\frac{\Delta t}{4}\mathbf{C}^{\mathrm{T}}\mathbf{D}_k\boldsymbol{\beta}+\mathbf{p}_{u,k}\right]$$

$$+\left(\delta \mathbf{d}_{k+1}^{\mathrm{T}}\right)\left[\mathbf{M}_d\frac{\mathbf{d}_{k+1}-\mathbf{d}_k}{\Delta t}-\mathbf{M}_{du}\left(\frac{\mathbf{u}_{k+1}-\mathbf{u}_k}{\Delta t}\right)+\frac{\Delta t}{4}\Delta\boldsymbol{\beta}-\frac{\Delta t}{2}\mathbf{g}_d+\frac{\Delta t}{4}\mathbf{B}\mathbf{C}\mathbf{u}_{k+1}-\mathbf{p}_{d,k+1}\right]$$

$$+\left(\delta \mathbf{d}_k^{\mathrm{T}}\right)\left[-\mathbf{M}_d\frac{\mathbf{d}_{k+1}-\mathbf{d}_k}{\Delta t}+\mathbf{M}_{du}\left(\frac{\mathbf{u}_{k+1}-\mathbf{u}_k}{\Delta t}\right)+\frac{\Delta t}{4}\Delta\boldsymbol{\beta}-\frac{\Delta t}{2}\mathbf{g}_d+\frac{\Delta t}{4}\mathbf{B}\mathbf{C}\mathbf{u}_k+\mathbf{p}_{d,k}\right]$$

$$+\left(\delta \boldsymbol{\beta}^{\mathrm{T}}\right)\frac{\Delta t}{4}\left[(\Delta\mathbf{d}_k+\mathbf{D}_k\mathbf{C}\mathbf{u}_k-\mathbf{s})+(\Delta\mathbf{d}_{k+1}+\mathbf{D}_{k+1}\mathbf{C}\mathbf{u}_{k+1}-\mathbf{s})\right]$$

$$(61)$$

Noting that $\delta S = 0$ and $\Delta\mathbf{d}_k+\mathbf{D}_k\mathbf{C}\mathbf{u}_k-\mathbf{s}=\mathbf{0}$ in terms of Eq. (50), we have

$$\begin{cases}\dfrac{\mathbf{M}_u}{\Delta t}(\mathbf{u}_{k+1}-\mathbf{u}_k)-\mathbf{M}_{du}^{\mathrm{T}}\left(\dfrac{\mathbf{d}_{k+1}-\mathbf{d}_k}{\Delta t}\right)+\dfrac{\Delta t}{2}\mathbf{h}_{\mathbf{u}_{k+1}}\mathbf{g}_h+\dfrac{\Delta t}{4}\mathbf{C}^{\mathrm{T}}\mathbf{D}_{k+1}\beta_k-\mathbf{p}_{u,k+1}=\mathbf{0} \\[2mm] -\dfrac{\mathbf{M}_u}{\Delta t}(\mathbf{u}_{k+1}-\mathbf{u}_k)+\mathbf{M}_{du}^{\mathrm{T}}\left(\dfrac{\mathbf{d}_{k+1}-\mathbf{d}_k}{\Delta t}\right)+\dfrac{\Delta t}{2}\mathbf{h}_{\mathbf{u}_k}\mathbf{g}_h+\dfrac{\Delta t}{4}\mathbf{C}^{\mathrm{T}}\mathbf{D}_k\beta_k+\mathbf{p}_{u,k}=\mathbf{0} \\[2mm] \mathbf{M}_d\dfrac{\mathbf{d}_{k+1}-\mathbf{d}_k}{\Delta t}-\mathbf{M}_{du}\left(\dfrac{\mathbf{u}_{k+1}-\mathbf{u}_k}{\Delta t}\right)-\dfrac{\Delta t}{2}\mathbf{g}_d+\dfrac{\Delta t}{4}\Delta\beta_k+\dfrac{\Delta t}{4}\mathbf{B}_k\mathbf{C}\mathbf{u}_{k+1}-\mathbf{p}_{d,k+1}=\mathbf{0} \\[2mm] -\mathbf{M}_d\dfrac{\mathbf{d}_{k+1}-\mathbf{d}_k}{\Delta t}+\mathbf{M}_{du}\left(\dfrac{\mathbf{u}_{k+1}-\mathbf{u}_k}{\Delta t}\right)-\dfrac{\Delta t}{2}\mathbf{g}_d+\dfrac{\Delta t}{4}\Delta\beta_k+\dfrac{\Delta t}{4}\mathbf{B}_k\mathbf{C}\mathbf{u}_k+\mathbf{p}_{d,k}=\mathbf{0} \\[2mm] \Delta\mathbf{d}_{k+1}+\mathbf{D}_{k+1}\mathbf{C}\mathbf{u}_{k+1}-\mathbf{s}=\mathbf{0}\end{cases}\quad(62)$$

Equation (62) is a system of nonlinear algebraic equations that can be solved using Newton's iteration method. If $\mathbf{M}_d$ and $\mathbf{M}_{du}$ in Eq. (62) are replaced with $\mathbf{M}_d\varepsilon$ and $\mathbf{M}_{du}\varepsilon$ ($\varepsilon \ll 1$), Eq. (62) can be used to analyze the shallow water problem ignoring the effect of the vertical velocity. In this case, the results are in agreement with the SVE solution.

4 Numerical examples

In this section, three classical numerical examples are used to verify the reliability of the proposed SWE-DP and the effectiveness of the proposed numerical method. These examples have been used frequently by many researchers to test different numerical methods [40–42].

4.1 Evolution of shorelines over a parabolic topography

The first example is a perturbed shallow water flow in a one-dimensional container with a parabolic bed profile, which provides a perfect test for the proposed method in dealing with bed sloping source term and wetting/drying condition. The analytical solutions for this problem were derived by Sampson et al. [40]. The initial water domain is shown in Fig. 3.

The bed profile is defined by

$$h(x) = h_0 - h_0\left(\frac{x}{a}\right)^2 \tag{63}$$

Fig. 3 The water profile at
$t = 0$ s
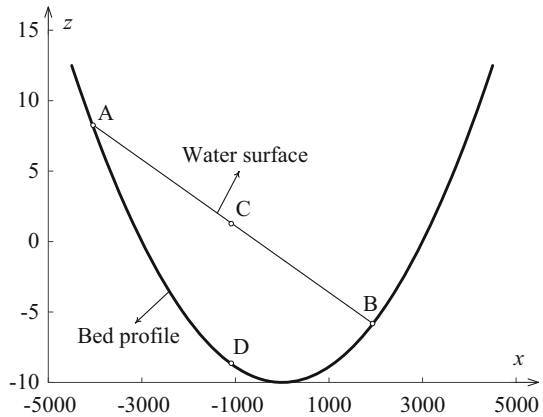
where $h_0 = 10$ m, and $a = 3000$ m. According to Ref. [40], the analytical horizontal displacement and water surface are shown as

$$u(x,t) = \frac{a^2}{2gh_0} B\omega(1 - \cos \omega t) \tag{64}$$

and

$$\eta(x,t) = -\frac{1}{g}B\omega \cos \omega t(x + u(x,t)) - \frac{a^2 B^2}{8g^2 h_0}\omega^2 \cos 2\omega t - \frac{B^2}{4g}, \quad \omega = \frac{\sqrt{2gh_0}}{a}, \tag{65}$$

respectively, in which the involved parameters are selected as $B = 5$ m/s, $g = 10$ m$/$s^2.

Numerical simulation is performed with a time step $\Delta t = 1$ s and a uniform grid with $N_e = 300$ elements. The simulation lasts for 6000 s. Figure 4 shows the predicted water surface elevation at different times. Figure 5 shows the predicted locations of the left and right shorelines. Excellent agreement is observed between the numerical prediction and analytical solutions from Figs. 4 to 5, which validates that the proposed method is able to address the shallow water with complex bed topographies and wet-dry interfaces.

The considered problem here is a conservative system, where the total energy of the system, denoted by $H(t)$, will keep constant with time. The total energy is the summation of the kinetic energy and the potential energy, i.e., $H(t) = T + U$. Figure 6 shows the relative error of the total energy, defined by $[H(t) - H_0]/H_0$, where $H_0 = H(0)$. This figure shows that the proposed method conserves precisely the discrete energy of the considered shallow water system over long times. The relative energy error is on the order of 10^{-10}.

Simulating the shallow water problem with wet-dry interfaces and a sloping bottom, the numerical solutions often cannot conserve the total mass of the system exactly. In [17], a zero mass error method was proposed by Brufau et al. Here the ability of the proposed method to conserve the mass is also tested. Figure 7 shows the relative error of the total mass of the system, denoted by $[m(t) - m_0]/m_0$, in which

$$m(t) = \rho \sum_{n=1}^{N_x} d_n(\Delta x_n + u_{n+1} - u_n) \tag{66}$$

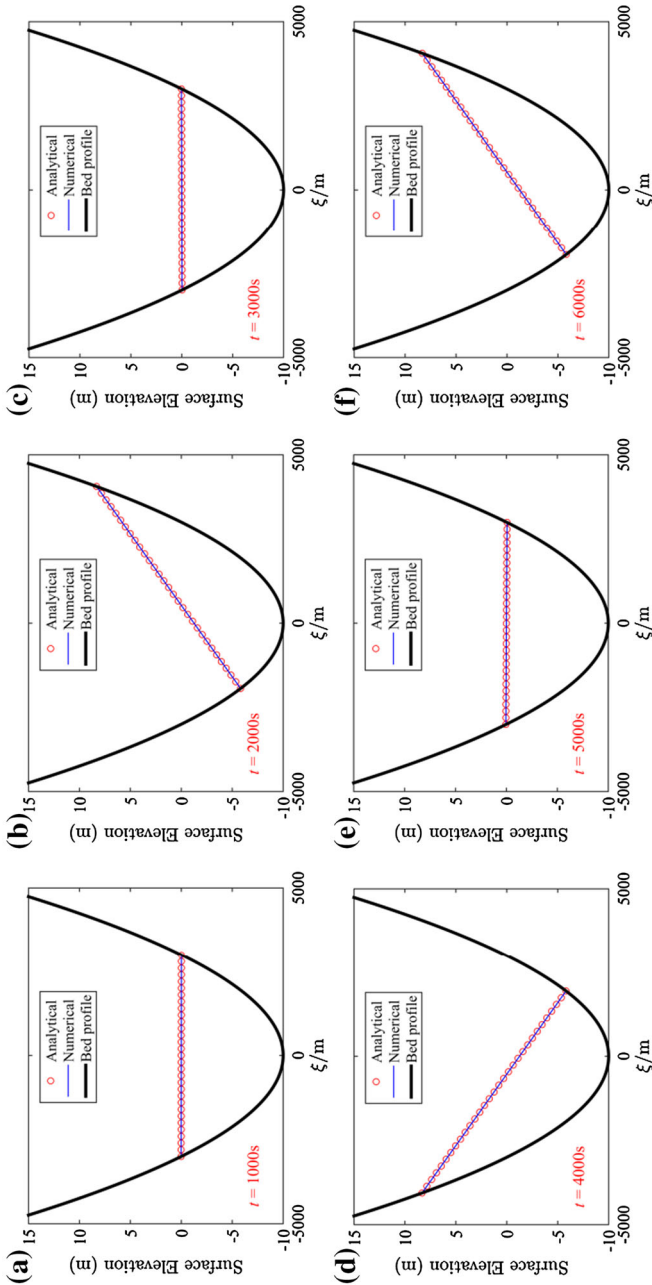is the total mass of the shallow water system, and $m_0 = m(0)$.

Fig. 4 Water surface elevation at different times: **a** $t = 1000$ s; **b** $t = 2000$ s; **c** $t = 3000$ s; **d** $t = 4000$ s; **e** $t = 5000$ s; **f** $t = 6000$ s

It can be observed from Fig. 7 that the relative mass error is on the order of 10^{-16}, which means that the proposed method can provide numerical results with zero mass errors.
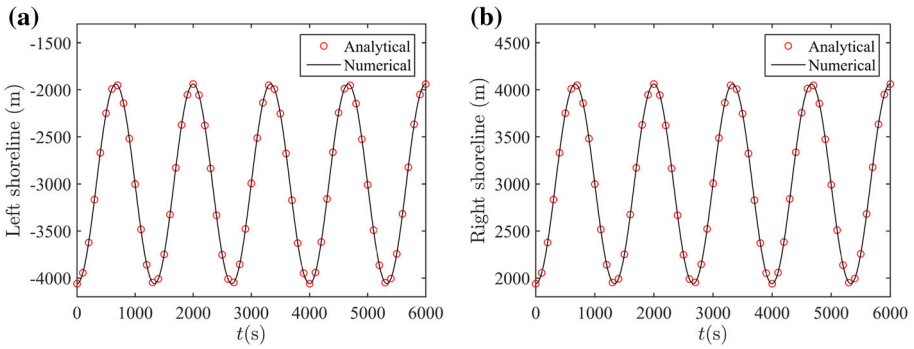
(a)

(b)

Fig. 5   Locations of shorelines: **a** Left shoreline; **b** Right shoreline

Fig. 6   Energy relative error, $[H(t) - H_0]/H_0$, for 6000 s
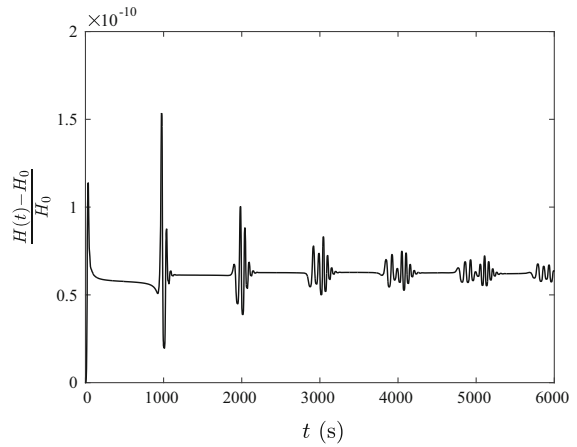
Fig. 7   Mass relative error, $[m(t) - m_0]/m_0$, for 6000 s
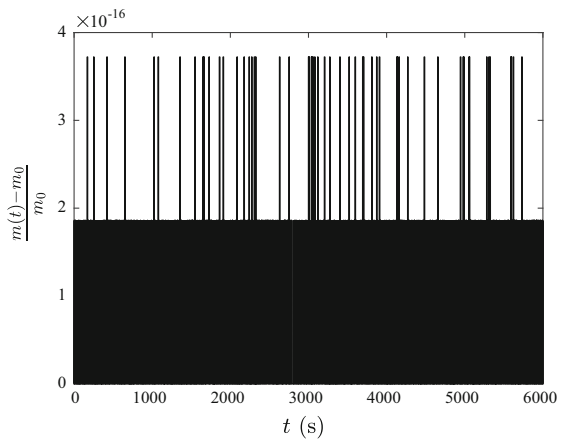
4.2 Spreading of a drop of shallow water

As the second example, the spreading of a parabola-shaped two-dimensional drop of shallow water on a horizontal plane is considered. The drop is initially confined to $|x| < 1$ according to

$$z = \eta_0(x) = \begin{cases} 1 - x^2 & \text{for } |x| < 1 \\ 0 & \text{for } |x| \geq 1, \end{cases} \tag{67}$$

and then is at rest. Upon releasing the drop, it spreads under the effect of gravity. The gravitational acceleration is $g = 1 \text{ m/s}^2$. The temporal evolution of this system has been analytically investigated by Frei [43]. He noted that the parabolic shape is always retained and that the velocity across the drop is a linear function, i.e.,

$$\eta(x,t) = \lambda^{-1}\left[1 - \left(\frac{\xi}{\lambda}\right)^2\right], \quad \dot{u}(x) = \xi\left(\frac{\lambda_t}{\lambda}\right) \tag{68}$$

in which, ξ is defined by Eq. (1), λ describes the half-width of the drop, and $\lambda_t = \partial\lambda/\partial t$ is the velocity of the leading edge. Following Refs. [43, 44], $\lambda(t)$ is obtained numerically as the root of the following equation

$$t = \frac{1}{2}\left[\sqrt{\lambda(\lambda-1)} + \ln\left(\sqrt{\lambda-1} + \sqrt{\lambda}\right)\right]. \tag{69}$$

The proposed SWE-DP is used to simulate this problem, and the numerical simulation is performed with $N_e = 100$ elements. The time step is selected as $\Delta t = 0.01$ s, and the numerical simulation lasts for 2 s. It is worth noting that the analytical solution (68) provided by Frei was derived based on the SVE, in which the effect of the vertical velocity is ignored. Hence in the numerical simulation, the matrices $\mathbf{M}_d$ and $\mathbf{M}_{du}$ in Eq. (62) are replaced with $0 \cdot \mathbf{M}_d$ and $0 \cdot \mathbf{M}_{du}$, respectively.

The analytical solutions and the numerical results computed using the proposed method are compared in Fig. 8. The first panel in Fig. 8 shows the comparison of the water free surfaces at 1 and 2 s, and the second panel in Fig. 8 shows the comparison of the velocities at 1 and 2 s. It can be observed that the numerical results computed using the proposed
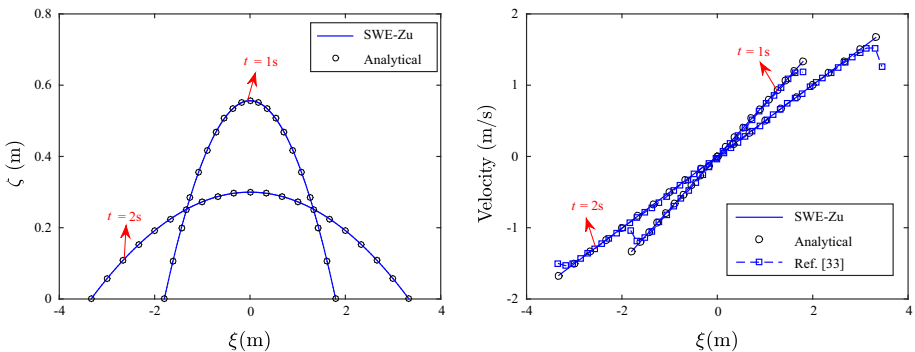

Fig. 8 Comparison between different solutions. *First panel* water free surfaces at 1 and 2 s; *Second panel*, velocities at 1 and 2 s

method are in excellent agreement with the analytical solution. The example used here was also discussed in Ref. [45], where the SVE was used to model the drop and a second order high resolution algorithm was applied to solve the SVE. The numerical velocities given in Ref. [45] are also displayed in the second panel of Fig. 8. It can be seen that these numerical velocities given in Ref. [45] are different from the analytical solutions at the left and right moving wet-dry interfaces, while the proposed method performs well at the wet-dry interfaces. Indeed, other researchers discussed this example by solving the SVE by means of different types of numerical schemes, e.g., Refs. [44, 46]. However, the accuracy of the numerical velocities at the left and right moving wet-dry interfaces in these reports was unsatisfactory. The numerical results demonstrate that the proposed model can correctly handle the problem of wet-dry interfaces.

In Fig. 9 the relative error of the total energy of the drop versus time is displayed. From Fig. 9 it may be observed that the relative energy error is on the order of 10^{-6}, which means that the proposed method conserves precisely the discrete energy of the considered shallow water system. The max relative error of the total mass for 2 s is on the order of 10^{-16}, and hence the relative error of the total mass versus time is not exhibited here.

4.3 Dam break on dry bed

Consider a reservoir with length 150 m and water depth 10 m; see Fig. 10. Suddenly, the right dam is broken and the water pours out of the reservoir. The right side of the dam is the dry bed. Initially, the water surface is defined as

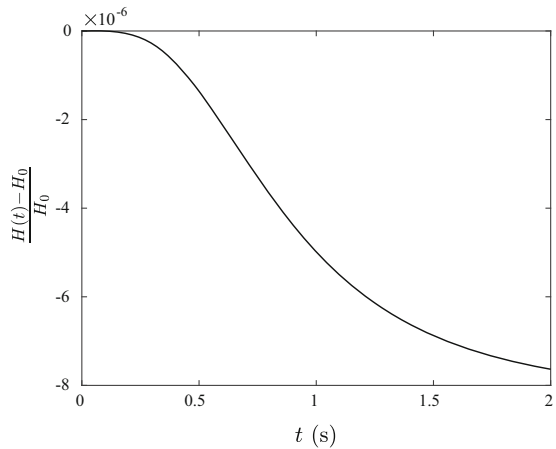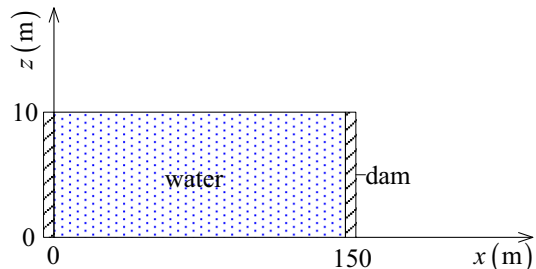**Fig. 9** Energy relative error, $[H(t) - H_0]/H_0$

Fig. 10 The dam

$$z = \eta_0(x) = \begin{cases} h_0, & \text{if } x \leq x_0 \\ 0, & \text{if } x > x_0, \end{cases} \tag{70}$$

where $x_0 = 150$ m and $h_0 = 10$ m. The initial velocity is $\dot{u}(x,0) = 0$ m/s, and the gravitational acceleration is $g = 9.81$ m/s.

According to Ref. [42], the analytical solution can be given as

$$\eta(x,t) = \begin{cases} h_0, & \text{if } \xi \leq x_0 - t\sqrt{gh_0} \\ \dfrac{1}{9g}\left(2\sqrt{gh_0} - \dfrac{\xi - x_0}{t}\right)^2, & \text{if } x_0 - t\sqrt{gh_0} < \xi \leq x_0 + 2t\sqrt{gh_0} \\ 0, & \text{if } \xi > x_0 + 2t\sqrt{gh_0} \end{cases} \tag{71}$$

and

$$\dot{u}(x,t) = \begin{cases} 0, & \text{if } \xi \leq x_0 - t\sqrt{gh_0} \\ \dfrac{2}{3}\left(\sqrt{gh_0} + \dfrac{\xi - x_0}{t}\right), & \text{if } x_0 - t\sqrt{gh_0} < \xi \leq x_0 + 2t\sqrt{gh_0} \\ 0, & \text{if } \xi > x_0 + 2t\sqrt{gh_0}, \end{cases} \tag{72}$$

where ξ is defined by Eq. (1).

It should be noted that in the analytical solutions (71) and (72) were derived based on the SVE, in which the effect of the vertical velocity is ignored. Hence, to test the reliability of the proposed SWE-DP and the correctness of the proposed numerical scheme, the matrices $\mathbf{M}_d$ and $\mathbf{M}_{du}$ in Eq. (62) are replaced with $0 \cdot \mathbf{M}_d$ and $0 \cdot \mathbf{M}_{du}$, respectively in the numerical simulation. Another numerical simulation considering the effect of the vertical velocity is also performed. Both these numerical simulations are performed with $N_e = 444$ elements and a time step of $\Delta t = 0.01$ s. The numerical simulation lasts for 6 s.

In Fig. 11, the water surface elevations and water discharges at $t = 6$ s computed using different methods are compared in the first and second panels, respectively. The black solid line represents the analytical solution. The red dash line represents the numerical results computed using the proposed method in the case of $\varepsilon = 0$, i.e., where the effect of the vertical velocity is ignored, and the blue dotted line represents the numerical results computed using the proposed method in the case of $\varepsilon = 1$, i.e., where the effect of the vertical velocity is considered.

Excellent agreement is observed between the numerical results of $\varepsilon = 0$ and the analytical solutions, from Fig. 11. No oscillations are detected in the computed results. This demonstrates the reliability of the proposed SWE-DP and the correction of the numerical scheme proposed in Sect. 4. It can also be observed from Fig. 11 that the vertical velocity makes the curves of the numerical results more smooth. Figure 12 shows the relative error of the total energy. It is clear that the proposed method conserves precisely the discrete energy. The relative energy error is on the order of 10^{-6}, and no numerical diffusion is detected in the computed results. The results depicted in these figures show that the proposed method is able to be employed to the shallow water problem with wet-dry interfaces.

Because the max relative error of the total mass for 6 s is on the order of 10^{-16}, the relative error of the total mass versus time is not exhibited here.
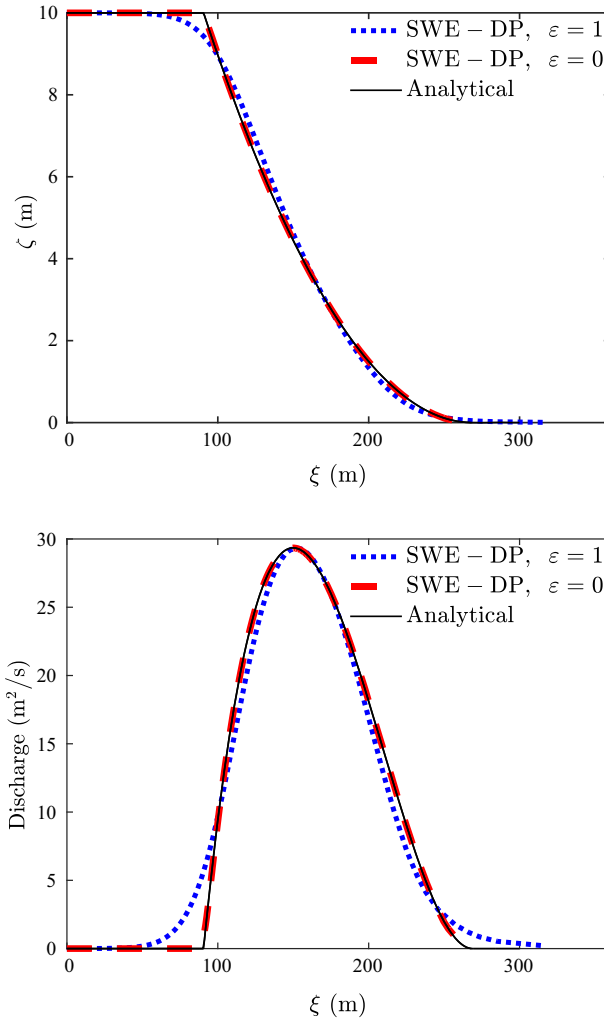
Fig. 11 Comparison between different solutions. *First panel* water free surfaces at 6 s; *Second panel*, water discharge at 6 s

4.4 Order of accuracy of the proposed scheme

The error of the proposed method depends on two factors, i.e., the mesh size and the time step. To analyze the order of accuracy of the proposed scheme, the example 4.1 is used. The effect of the mesh size on the proposed method is discussed first by using different mesh sizes and the same time step. We select four quantities, i.e., u_A, u_B, d_C and β_D, to determine the order of accuracy. Here, u_A and u_B represent the displacements at the points A and B, respectively. d_C is the water depth at the point C, and β_D the pressure at the point D. The points A, B, C, and D are shown in Fig. 3. The x coordinate values of the points A and B are -4060.66 m and 1939.34 m. The x coordinate values of the points C and D are both -1060.66 m. Points A and B are the initial left shoreline and right shoreline,
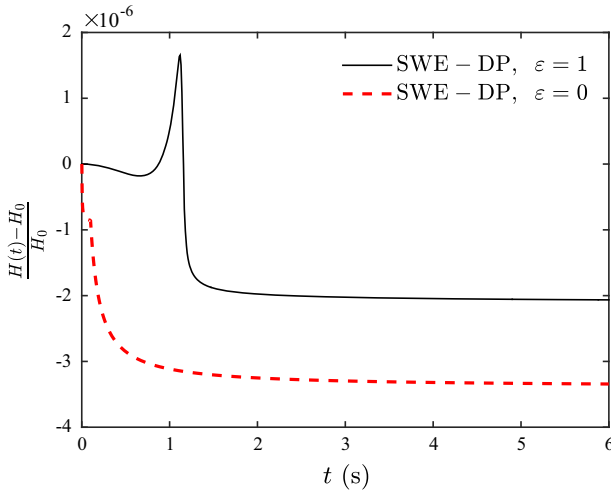
Fig. 12 Energy relative error for 6 s

respectively. Points C and D are located at the water surface and bottom, respectively. Let the numerical error be defined by

$$e(y) = \frac{\sum\limits_{i=1}^{N_t} |y(t_i) - y^*(t_i)|}{\sum\limits_{i=1}^{N_t} |y^*(t_i)|} \tag{73}$$

where $y(t_i)$ are the solutions at time t_i computed using different mesh sizes, and $y^*(t_i)$ are the reference solutions at time t_i. N_t is the number of time steps. The numerical error can be expressed as $e = C\Delta x^s$, in which C is a constant independent of the mesh size Δx, and s is the order of accuracy associated with the mesh size. Thus, the errors e_1 and e_2 for two different mesh sizes Δx_1 and Δx_2 can be given by

$$e_1 = C\Delta x_1^s, \quad e_2 = C\Delta x_2^s, \tag{74}$$

and the order of accuracy can be shown by

$$s = \frac{\log_{10}(e_1) - \log_{10}(e_2)}{\log_{10}(\Delta x_1) - \log_{10}(\Delta x_2)}. \tag{75}$$

Three different mesh sizes $\Delta x_1 = 60$ m, $\Delta x_2 = 30$ m, $\Delta x_3 = 30$ m and $\Delta x_4 = 15$ m are selected to determine the order of accuracy in space. The solutions with mesh size Δx_4 are

Table 1 The effect of the mesh size on the convergence rate

	u_A	u_B	d_C	β_D
e_1	1.645E−02	1.663E−02	7.106E−04	7.107E−04
e_2	5.566E−03	5.628E−03	2.211E−04	2.213E−04
e_3	1.930E−03	1.952E−03	1.010E−04	1.011E−04
Order	2.088	2.088	1.809	1.808

Table 2 The effect of the time step on the convergence rate

	$\mathbf{u}(t_1)$	$\mathbf{u}(t_2)$	$\mathbf{u}(t_3)$	$\mathbf{d}(t_1)$	$\mathbf{d}(t_2)$	$\mathbf{d}(t_3)$	$\boldsymbol{\beta}(t_1)$	$\boldsymbol{\beta}(t_2)$	$\boldsymbol{\beta}(t_3)$
e_1	4.01E−05	1.22E−04	1.80E−04	1.39E−05	9.77E−05	1.72E−04	1.17E−05	9.22E−05	1.70E−04
e_2	9.23E−06	2.99E−05	4.72E−05	3.11E−06	2.27E−05	5.59E−05	2.34E−06	2.02E−05	5.18E−05
e_3	1.83E−06	5.95E−06	9.58E−06	5.90E−07	4.25E−06	1.16E−05	4.35E−07	3.53E−06	1.04E−05
Order	2.23	2.18	2.12	2.28	2.26	1.94	2.37	2.35	2.02

seen as the reference solution. The time step is $\Delta t = 1$ s, and the interval of the time integration is set to be $[0, 6000]$ s. The numerical errors e_i ($i = 1 \sim 3$) of u_A, u_B, d_C and β_D are listed in Tables 1, in which e_i represents the numerical error calculated by using the mesh size Δx_i. The orders of accuracy in space, calculated by the use of Eq. (75), are also listed in this table.

From Table 1, it can be seen that the numerical errors decrease as the mesh size gradually decreases, and the order of accuracy associated with the mesh size is approximately 2.

Next, we test the effect of the time step on the accuracy of the proposed method by using different time steps and the same mesh size. Let the numerical error be defined by

$$e(\mathbf{y}(t)) = \frac{\|\mathbf{y}(t) - \mathbf{y}^*(t)\|_1}{\|\mathbf{y}^*(t)\|_1} \tag{76}$$

where $\mathbf{y}(t)$ are the displacement and pressure vectors computed using different time steps, and $\mathbf{y}^*(t)$ is the reference solutions. The numerical error can also be expressed as $e = C\Delta t^l$, in which C is a constant independent of the time step Δt and l is the order of accuracy associated with the time step. For two different time steps Δt_1 and Δt_2, the errors are

$$e_1 = C\Delta t_1^l, \quad e_2 = C\Delta t_2^l, \tag{77}$$

and the order of accuracy can be expressed as

$$l = \frac{\log_{10}(e_1) - \log_{10}(e_2)}{\log_{10}(\Delta t_1) - \log_{10}(\Delta t_2)}. \tag{78}$$

Four time steps $\Delta t_1 = 2$ s, $\Delta t_2 = 1$ s, $\Delta t_3 = 0.5$ s, and $\Delta t_4 = 0.25$ s are selected and the solutions computed using the smallest time step are seen as the reference solutions. The mesh size is $\Delta x = 20$ m. The numerical errors e_i ($i = 1 \sim 3$) of $\mathbf{u}(t)$, $\mathbf{d}(t)$, and $\boldsymbol{\beta}(t)$ at times $t_1 = 1000$ s, $t_2 = 3000$ s and $t_3 = 5000$ s are listed in Tables 2, in which e_i represents the numerical error calculated by using the time step Δt_i. The orders of accuracy in time, calculated by the use of Eq. (78), are also listed in Table 2.

From Table 2, it can be seen that the numerical errors decrease as the time step gradually decreases, and the order of accuracy associated with the time step is approximately 2. In terms of Tables 1 and 2, it is possible to conclude that the accuracy of the proposed method is second order.

5 Conclusion

The Lagrange method and the constrained Hamilton variational principle in classical mechanics are used for the shallow water wave problem with a sloping bottom and wet-dry interface. Based on the constrained Hamilton variational principle, a shallow water equation based on the displacement and pressure (SWE-DP) has been presented. A hybrid numerical method combining the finite element method for spatial discretization and the symplectic Zu-class method for time integration is constructed for the SWE-DP. Three numerical examples are used to test the reliability of the proposed SWE-DP and the effectiveness of the hybrid numerical method proposed for the SWE-DP. Numerical examples show that the proposed method performs well in the simulation of shallow water with a sloping bottom and wet-dry interface.

In this paper, we only consider one-dimensional shallow water. However, the basic ideas can be expanded to other hydrodynamics problems. Though the Eulerian coordinate system is the most popular approach in hydrodynamics, the Lagrangian coordinate system can be seen as an efficient supplementary approach based on its advantages of satisfying exactly nonlinear boundary conditions, such as the free surface orwetting/drying condition. We believe that the displacement method will play an important role in accurately and efficiently simulating hydrodynamics problems. In our next work, the proposed method will be expanded to shallow water with two dimensions.

Appendix: Relation with the SWEs in the Euler description

Let the flow velocity in the Euler description be denoted by $V(\xi, t)$. In terms of Eq. (1), we have

$$\frac{\partial}{\partial x} = (1 + u_x)\frac{\partial}{\partial \xi} \tag{79}$$

and

$$\begin{aligned} \bar{d}(\xi, t) = \bar{d}(x + u(x,t), t) = d(x,t) \\ \bar{u}(\xi, t) = \bar{u}(x + u(x,t), t) = u(x,t), \end{aligned} \tag{80}$$

where $\bar{\#}(\xi)$ denotes the variable in the Euler description. The Lagrangian acceleration can be expressed as

$$\ddot{u}(x) = \frac{\partial V(\xi, t)}{\partial t} + V\frac{\partial V(\xi, t)}{\partial \xi}. \tag{81}$$

In terms of Eqs. (1) and (16), we have

$$\bar{h}_x = \frac{\partial h(a)}{\partial a}\bigg|_{a = x + u} = \frac{\partial h(\xi)}{\partial \xi}. \tag{82}$$

Substituting Eqs. (81) and (82) into the first equation of Eq. (37) and noting Eq. (79), we have

$$\rho d_0 \left(\frac{\partial V(\xi, t)}{\partial t} + V\frac{\partial V(\xi, t)}{\partial \xi}\right) - \rho g d_0 \frac{\partial h(\xi)}{\partial \xi} + \frac{1}{2}\frac{\partial(\beta d)}{\partial x} = 0. \tag{83}$$

In terms of the second and third equations of Eq. (37), we can obtain the following equations

$$\frac{\partial \xi}{\partial x} = u_x + 1 = \frac{d_0}{d(x,t)} = \frac{d_0}{\bar{d}(\xi, t)}, \tag{84}$$

and

$$\beta = \rho g \frac{d_0}{(1 + u_x)} = \rho g \bar{d}(\xi, t). \tag{85}$$

Substituting Eqs. (84) and (85) into Eq. (83) yields

$$\frac{\partial V(\xi,t)}{\partial t} + V\frac{\partial V(\xi,t)}{\partial \xi} + g\frac{\partial \bar{d}}{\partial \xi} = g\frac{\partial h(\xi)}{\partial \xi}. \tag{86}$$

Meanwhile, the derivative of (84) with respect to time is

$$\dot{u}_x d(x,t) + (1+u_x)\dot{d}(x,t) = 0. \tag{87}$$

Noting that

$$\dot{u}_x = \frac{\partial \dot{u}(x)}{\partial x} = \frac{\partial V(\xi)}{\partial x} = \frac{\partial V}{\partial \xi}(1+u_x), \tag{88}$$

and

$$\frac{\partial d}{\partial t} = \frac{\partial \bar{d}}{\partial t} + \frac{\partial \bar{d}}{\partial \xi}V, \tag{89}$$

Equation (87) can be further rewritten as

$$\frac{\partial \bar{d}}{\partial t} + \frac{\partial (V\bar{d})}{\partial \xi} = 0. \tag{90}$$

Eqs. (86) and (90) constitute the SVE in the Euler description,

$$\begin{cases} \dfrac{\partial V(\xi,t)}{\partial t} + V\dfrac{\partial V(\xi,t)}{\partial \xi} + g\dfrac{\partial \bar{d}}{\partial \xi} = g\dfrac{\partial h(\xi)}{\partial \xi} \\ \dfrac{\partial \bar{d}}{\partial t} + \dfrac{\partial (V\bar{d})}{\partial \xi} = 0. \end{cases} \tag{91}$$

The above analysis means that the proposed SWE-DP is mathematically equivalent to the SVE when the effect of the vertical velocity is ignored.

Equation (37) can also be expressed in the conservative form. Introduce the two variables:

$$p_u = \rho d_0 \dot{u}, \quad \gamma = d_0/d \tag{92}$$

where p_u is the moment in the x-direction, and γ is a dimensionless parameter, that is the ratio of the water depths at times 0 and t. Using Eqs. (38) and (92), the first equation in Eq. (37) can be rewritten as

$$\frac{\partial p_u}{\partial t} + \frac{\partial}{\partial x}\left(\frac{\rho g d_0^2}{2\gamma^2}\right) = \rho g d_0 \bar{h}_x. \tag{93}$$

In terms of Eq. (92), the incompressible equation, i.e., the third equation in Eq. (37), can be rewritten as

$$\gamma = 1 + u_x \tag{94}$$

Noting from Eq. (92) that $\dot{u} = p_u/(\rho d_0)$, the partial derivative of Eq. (94) with respect to t yields

$$\frac{\partial \gamma}{\partial t} = \frac{\partial u_x}{\partial t} = \frac{\partial (u_t)}{\partial x} = \frac{\partial}{\partial x}\left(\frac{p_u}{\rho d_0}\right) \tag{95}$$

Hence, Eq. (37) can be expressed as the following conservative form

$$\begin{cases} \dfrac{\partial p_u}{\partial t} + \dfrac{\partial}{\partial x}\left(\dfrac{\rho g d_0^2}{2\gamma^2}\right) = \rho g d_0 \bar{h}_x \\ \dfrac{\partial \gamma}{\partial t} + \dfrac{\partial}{\partial x}\left(\dfrac{-p_u}{\rho d_0}\right) = 0 \end{cases} \tag{96}$$

The first equation in Eq. (96) represents the momentum conservation equation, and the second one represents the mass conservation equation. However, it can be observed by comparison with Eq. (91) that there is no so-called convection term in Eq. (96).

References

1. Vreugdenhil CB (1994) Numerical methods for shallow-water flow. Springer, Netherlands
2. Winters AR, Gassner GJ (2015) A comparison of two entropy stable discontinuous Galerkin spectral element approximations for the shallow water equations with non-constant topography. J Comput Phys 301:357–376
3. Khan AA, Lai WC (2014) Modeling shallow water flows using the discontinuous Galerkin method. CRC Press, New York
4. Dehghan M, Salehi R (2012) A meshless based numerical technique for traveling solitary wave solution of Boussinesq equation. Appl Math Model 36(5):1939–1956
5. Dumbser M, Facchini M (2016) A space-time discontinuous Galerkin method for Boussinesq-type equations. Appl Math Comput 272:336–346
6. Ortiz P (2012) Non-oscillatory continuous FEM for transport and shallow water flows. Comput Method Appl M 223–224:55–69
7. Feng J, Cai L, Xie W (2006) CWENO-type central-upwind schemes for multidimensional Saint-Venant system of shallow water equations. Appl Numer Math 56(7):1001–1017
8. Guo Y, Liu R, Duan Y et al (2009) A characteristic-based finite volume scheme for shallow water equations. J Hydrodyn 21(4):531–540
9. Bo LH, Jin S (2009) Study on high resolutio scheme for shallow water equation with source terms. J Hydrodyn Ser A 24(01):22–28
10. Liang Q, Marche F (2009) Numerical resolution of well-balanced shallow water equations with complex source terms. Adv Water Resour 32(6):873–884
11. Bermudez A, Ma EV (1994) Upwind methods for hyperbolic conservation laws with source terms. Comput Fluids 23(8):1049–1071
12. Duran A, Liang Q, Marche F (2013) On the well-balanced numerical discretization of shallow water equations on unstructured meshes. J Comput Phys 235:565–586
13. Zhao LH, Guo BW, Li TC et al (2014) A well-balanced explicit/semi-implicit finite element scheme for shallow water equations in drying-wetting areas. Int J Numer Meth Fl 75(12):815–834
14. Amiri SM, Talebbeydokhti N, Baghlani A (2013) A two-dimensional well-balanced numerical model for shallow water equations. Sci Iran 20(1):97–107
15. Alemi Ardakani H, Bridges TJ, Turner MR (2016) Shallow-water sloshing in a moving vessel with variable cross-section and wetting–drying using an extension of George's well-balanced finite volume solver. J Comput Phys 314:590–617
16. Marche F, Bonneton P, Fabrie P et al (2007) Evaluation of well-balanced bore-capturing schemes for 2D wetting and drying processes. Int J Numer Meth Fl 53(5):867–894
17. Brufau P, Garcia-Navarro P, Vázquez-Cendón ME (2004) Zero mass error using unsteady wetting–drying conditions in shallow flows over dry irregular topography. Int J Numer Method Fluids 45:1047–1082
18. Chen Y, Hsu H (2009) A third-order asymptotic solution of nonlinear standing water waves in Lagrangian coordinates. Chinese Phys B 18(3):861–871

19. Stoker JJ (1957) Water waves: the mathematical theory with applications. Interscience Publishers LTD, New York
20. Tao MD (1990) The Sudden starting of a floating body in deep water. Appl Math Mech 11(02):149–154 **(English Edition)**
21. Tao MD, Shi XM (1993) Problem of hydrodynamic pressure on suddenly starting vessel. Appl Math Mech 14(02):151–158 **(English Edition)**
22. Shi XM, Le JC, Ping AS (2002) Nonlinear wave induced by an accelerating cylindrical tank. J Hydrodyn Ser B 14(02):12–16 **(English edition)**
23. Morrison PJ, Lebovitz NR, Biello JA (2009) The Hamiltonian description of incompressible fluid ellipsoids. Ann Phys-New York 324(8):1747–1762
24. Lu DQ, Dai SQ, Zhang BS (1999) Hamiltonian formulation of nonlinear water waves in a two-fluid system. Appl Math Mech-Engl 20(4):343–349
25. Suzuki Y, Koshizuka S, Oka Y (2007) Hamiltonian moving-particle semi-implicit (HMPS) method for incompressible fluid flows. Comput Method Appl M 196(29–30):2876–2894
26. Kheiri M, Païdoussis MP (2014) On the use of generalized Hamilton's principle for the derivation of the equation of motion of a pipe conveying fluid. J Fluid Struct 50:18–24
27. Wang Y, Deng ZC, Hu WP (2014) Symplectic exact solution for stokes flow in the thin film coating applications. Math Probl Eng 2014:1–12
28. Zienkiewicz OC, Taylor RL (2000) Finite element method. Butterworth-Heinemann, Oxford
29. Feng K, Qin MZ (2010) Symplectic geometric algorithms for hamiltonian systems. Springer, Berlin
30. Tanaka N, Kitayama T (2004) Symplectic semi-Lagrangian schemes for computational fluid dynamics. Int J Comput Fluid D 18(4):303–308
31. Wu F, Zhong WX (2016) Constrained Hamilton variational principle for shallow water problems and Zu-class symplectic algorithm. Appl Math Mech Engl 37(1):1–14
32. Liu P, Li Z, Luo R (2012) Modified (2 + 1)-dimensional displacement shallow water wave system: symmetries and exact solutions. Appl Math Comput 219(4):2149–2157
33. Liu P, Fu PK (2011) Modified (2 + 1)-dimensional displacement shallow water wave system and its approximate similarity solutions. Chin Phys B 20(0902039):90203
34. Liu P, Lou SY (2008) A (2 + 1)-dimensional displacement shallow water wave system. Chin Phys Lett 25(9):3311–3314
35. Zhong WX (2006) Symplectic method in applied mechanics. High Education Press, Beijing
36. Zhong WX, Gao Q (2006) Integration of constrained dynamical system via analytical structural mechanics. J Dyn Control 4(03):193–200
37. Zhong WX, Gao Q, Peng HJ (2013) Classical mechanics—its symplectic description. Dalian University of Technology Press, Dalian
38. Wu F, Zhong WX (2015) The Zu-type method is symplectic. Chin J Comput Mech 32(4):447–450
39. Arnol'd VI (1997) Mathematical methods of classical mechanics. Springer, New York
40. Sampson J, Easton A, Singh M (2005) Moving boundary shallow water flow above parabolic bottom topography. Anziam J 47:373–387
41. Murillo J, García-Navarro P (2012) Augmented versions of the HLL and HLLC Riemann solvers including source terms in one and two dimensions for shallow flow applications. J Comput Phys 231(20):6861–6906
42. Izem N, Seaid M, Wakrim M (2016) A discontinuous Galerkin method for two-layer shallow water equations. Math Comput Simul 120:12–23
43. Frei C (1993) Dynamics of a two-dimensional ribbon of shallow water on a f-plane. Tellus A 45(1):44–53
44. Sch RC, Smolarkiewicz PK (1996) A synchronous and iterative flux-correction formalism for coupled transport equations. J Comput Phys 128(1):101–120
45. Bo LH (2013) Study on the shallow water euqations of high resolution algorithm. Dissertation, Dalian University of Technology
46. Jarecka D, Jaruga A, Smolarkiewicz PK (2015) A spreading drop of shallow water. J Comput Phys 289:53–61